A computational study of the influence of the gallium doping atom of the germanium clusters: the geometries, electronic, and magnetic characteristics

IKRAM ZITOUNI*, OMAR BENTOUILA, KAMAL EDDINE AIADI, MERIEM BENAIDA, ZAHIA AYAT
Laboratoire de Développement des Energies Nouvelles et Renouvelables en Zones Aride, Université de Ouargla, 30000 Ouargla, Algeria

A theoretical systematic investigation of $GaGe_n$ clusters (n = 1–20) was presented within the framework of the DFT as implemented in the SIESTA simulation code. In order to study the relative stability of $GaGe_n$ clusters, we calculated the fragmentation energies, second-order difference of energies, binding energies, HOMO-LUMO gaps, vertical electron affinity, vertical ionization potential, and total spin magnetic moment. The results of the electronic properties calculations reveal that the $GaGe_1$ dimer is more suitable than neighboring cluster sizes. We obtained that all the lowest-energy of $GaGe_n$ clusters have magnetic structures, where the $GaGe_1$ has a higher total spin magnetic moment.

(Received February 25, 2021; accepted December 6, 2022)

Keywords: DFT method, Spin polarized calculations, Germanium clusters, Geometry, Gallium-doped germanium clusters

1. Introduction

Nanotechnology uses small structures, these latter contain nano-particles which their dimensions are less than one hundred nanometers. Often their chemical and physical properties differ from those of materials on a larger scale [1]. In addition, good knowledge of the properties of materials plays a very important role in controlling the manufacture of electronic devices, and also in discovering new materials and nano-structures with interesting new properties [2]. In this context, many computational and experimental researches have been extensively investigated in recent years aiming to find the physical and chemical properties of semiconductor clusters in their pure and doped state [3-13].

Recently, the semiconductor cluster "germanium" has emerged as a promising candidate for replacing silicon in advanced electronic components and its applications [14].

The $TMGe_n$ clusters have been extensively studied [15]. For instance, $FeGe_n$ (n = 9–16) clusters were studied by Zhao and Wang in 2008 [9]. The authors arrived at that the replacement of one Ge by one atom of Fe contributed in the reinforcement of the stability for the germanium framework. Deng et al. [10] have investigated the $CoGe_n^q$ (q = 0, ±1) (n = 2–11) clusters, and figured out that the magnetic moments of the charged $CoGe_n$ clusters decreased at n = 10 and 11.

By using the density functional theory (DFT) the structures, electronic and magnetic characteristics were calculated of the following clusters: $MoGe_n$ (n = 1–20) [11], $CoGe_n$ (n = 1–13) [12], $Bi_2Ge_n^{-2}$ (n = 3–8, 12) [13], and Sn_mGe_n (m + n ≤ 5) [14]. These studies depend on the nature of the doping material as well as on the size and structure of the cluster. Where they point out that the doping of the Co atom reinforcement the stability of the pure germanium framework, and the $CoGe_{10}$ cluster with the bicapped tetragonal antiprism configuration has more stability as compared to other clusters [12]. The larger-sized Ge and Sn clusters have higher binding energy and larger HOMO–LUMO energy gaps. This signifies that they are more stable [14].

The calculations based on DFT theory done by Benaida et al. [16] aim to find the physicochemical characteristics of pure germanium Ge_{n+1} and $AsGe_n$ clusters. They established that arsenic doping takes a surface situation in all cases.

Mahtout et al. [17–20] conducted several extensive studies on metal-doped germanium clusters according to the density functional theory computations. For $CrGe_n$ (n = 15–29) clusters, they found that the $CrGe_n$ clusters with sizes n = 20, 23 and 26 atoms have the largest value of chemical hardness, also they found that the $CrGe_{19, 24}$ clusters have the lowest value of the total spin magnetic moment and the $CrGe_{18}$ cluster has the highest value of that [17]. In the case of MGe_n (M = Au, Cu, Ag and n = 1 to19), the endohedral frame was obtained when the metal atom was encapsulated inside the Ge_{n+1} cage and it appears at n = 10 for Cu doping atom and at n = 12 for both Au and Ag [18]. In addition, very recently have been discussed the effect of platinum and palladium atoms on characteristics of Ge_n cage clusters (M = Pt, Pd and n = 1 to 20) [21], where both Pt and Pd structures have great stability of n = 10, 12, 16, and 18 atoms. These studies [17, 18, 21] proved that doping using one metal atom enhances the stability of germanium structure.

In this research, we have been studied and calculated the physical and chemical characteristics of $GaGe_n$ clusters with the ranges of large size (n = 1–20) by using the DFT method. We seek to demonstrate the influence of the gallium doping atom on the physicochemical properties of different isomers of germanium clusters and describe their evolution as a function of the cluster size.

In section 2 of this paper, a brief description of the calculation methodology for the studied system ($GaGe_n$ clusters, n = 1–20) is presented. Section 3 shows the results and their discussion. Finally, in the last section, we provide some main conclusions.

2. Computational methods

We applied our computational study in the SIESTA packages [22] using the norm conserving Troullier-Martins pseudopotentials [23], within the density functional theory (DFT) [24] with generalized gradient approximation [25]. The geometric configurations are optimized by using the conjugate gradient method until the residual forces were less than 10^{-3} eV/Å. Also, the k grid integration was executed by using the gamma-point (Γ) approximation. Besides, the self-consistent calculations with a convergence criterion of 10^{-4} a.u for the system's total energy have been employed. In our calculation, we chose a cubic supercell of 40 Å length to evade interactions among adjacent clusters, and we utilized the double ζ (DZ) basis for both Ga and Ge atoms.

In this our research, we determined the putative forms of $GaGe_n$ (n = 1 to 20) by replacement of one Ge atom by a Ga one in distinct sites of the host pure germanium isomers to obtain more stable structures for presentation and discussion. While in previous work [16], several possibilities of pure germanium isomers were relaxed.

The reliability of the calculation method was verified based on the results of the calculations on Ge_2 and Ga_2 clusters, where it was found that our results are in agreement with the previous theoretical and experimental results (as shown in Table 1).

Table 1. Averaged bond length a (Å) and binding energy E_b (eV) for Ge_2 and Ga_2 clusters compared to the available experimantal and theoretical data

Cluster	Our work		Bibliography data	
	a(A^0)	E_b(eV)	a(A^0)	E_b(eV)
Ge_2	2.503	1.445	2.450[a]	1.230[e]
			2.570[b]	1.440[a]
			2.440[c]	1.340[c]
			2.420[d]	1.350[f]
Ga_2	2.887	0.790	2.716[g]	1.053[l]
			2.762 [h, i]	
			2.715 [h]	
			2.810 [j, k, l]	

[a] Ref. [18]. [b] Ref. [26]-Expt. [c] Ref. [6]. [d] Ref. [7]. [e] Ref. [27]. [f] Ref. [8]-Expt. [g] Ref. [28]. [h] Ref. [29]. [i] Ref. [30]. [j] Ref. [31]. [k] Ref. [32]-Expt. [l] Ref. [33].

3. Results and discussion

3.1. Geometrical structures properties

In this section, we investigated and structurally analyzed the geometric structures obtained. This is primarily based on the atomic positions, the inter-atomic distances, and the symmetries. Where we determined the putative lowest-energy structure from a large number of isomers calculated. These most stable structures are shown in Fig. 1. Also, the values of the computed physical parameters are tabulated in Table 2.

We found that the binding energy (per atom) and the bond length of the GaGe dimer equal 1.219 eV and 2.631Å, respectively.

The most favorable geometry of $GaGe_2$ trimer displays a triangular frame with C_{2v} point group symmetry, where it has the binding energy of 1.737 eV/atom, which is lower compared to that of pure Ge_3 trimer [16]. For the size n = 3, the most stable structure of the $GaGe_3$ cluster takes a planar geometry with bond lengths of 2.604 Å and 2.735 Å for Ge–Ge and Ga–Ge respectively. Their calculated binding energy equal to 2.258 eV/atom, and it is least than that of a pure Ge_4 cage (2.707 eV/atom) [16].

The pentamer $GaGe_4$ exhibits a structure that contained 3 triangles with symmetry C_1. The mentioned structure has the average Ge–Ge and Ga–Ge bond lengths are 2.594 Å and 2.896 Å, respectively.

In the case cluster n = 5, the gallium atom is capping the structure of pure Ge_5, this latter can be named as a triangular pyramid [16]. Average Ga–Ge and Ge–Ge bond lengths of $GaGe_5$ are 2.701 Å and 2.734 Å, respectively.

The ground state of $GaGe_6$ isomer reveals a C_s bicapped pentagonal forme. It has a binding energy of 0.265eV/atom, which is somewhat smaller than that of Ge_7 frame [16].

The lowest-energy isomers for $GaGe_{7,8}$ clusters have a capped pentagonal bipyramid structures with symmetry C_1 and C_s respectively. These configurations similar to the structures of both $Ge_{8,9}$ clusters [16].

A capped pentagonal shape (C_{3v}) is established to be the most appropriate isomer for $GaGe_9$. Where its binding energy is 2.923 eV/atom. The Ga–Ge and Ge–Ge have average bond lengths equals to 2.876 Å and 2.816 Å, respectively.

Regarding the $GaGe_{10}$ cluster, the most suitable shape has a C_s point group symmetry, where gallium doping atom takes a peripheral position of the $GaGe_{10}$ structure. The Ga–Ge average distance in $GaGe_{10}$ cluster is 0.133 Å which is larger than that of the isomer for $GaGe_9$.

In addition, the prolate shape (C_1) of ground state isomer $GaGe_{11}$ is observed where Ga atom takes a stable position in the surface of the germanium frame. This shape has a calculated binding energy of 2.917 eV/atom.

For the size n = 12, in order to obtain the most suitable configuration, it replaced the capping germanium atom with the tetrahedral coordination by one gallium atom. The found values of the average distance Ge–Ge and Ga–Ge are 2.812 Å and 2.842 Å, respectively.

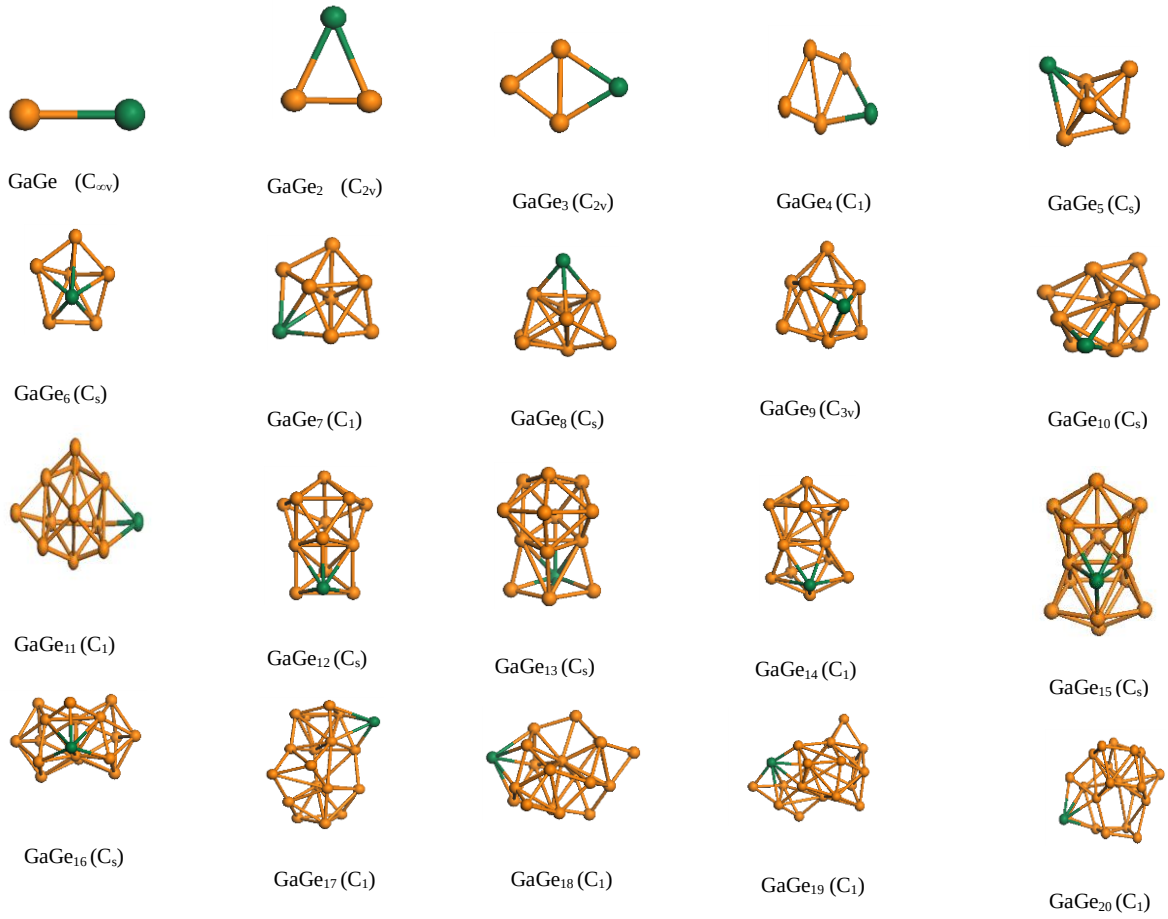

Fig. 1. Most stable geometries for $GaGe_n$ (n = 1–20) clusters (color online)

Table 2. Symmetry group, binding energy Eb (eV), HOMO-LUMO gap ΔE (eV), total spin magnetic moment μ (μ_B), vertical electron affinity VEA (eV), vertical ionization potential VIP (eV), chemical hardness η (eV), and average bond length $a_{Ge\text{-}Ge}$ (Å) and $a_{Ga\text{-}Ge}$ (Å) for $GaGe_n$ (n = 1–20) clusters

Cluster size (n)	symmetry	E_b(eV/atom)	ΔE (eV)	μ (μ_B)	VEA (eV)	VIP (eV)	η (eV)	$a_{Ge\text{-}Ge}$ (Å)	$a_{Ga\text{-}Ge}$ (Å)
1	a-$C_{\infty v}$	1.219	2.222	3.000	0.735	7.749	7.014	-	2.631
2	a- C_{2v}	1.737	0.466	0.999	1.832	7.674	5.842	2.297	3.017
3	a-C_{2v}	2.258	1.110	0.999	1.714	7.702	5.988	2.604	2.735
4	a -C_1	2.402	0.984	0.999	1.257	7.912	6.655	2.594	2.896
5	a-C_s	3.148	0.657	0.999	1.983	7.796	5.813	2.734	2.701
6	a-C_s	2.692	0.556	0.999	2.803	8.065	5.262	2.731	2.900
7	a-C_1	2.761	0.767	0.999	1.655	8.199	6.544	3.163	3.012
8	a-C_s	2.827	0.744	0.999	2.317	7.481	5.164	2.797	2.960
9	a- C_{3v}	2.923	0.438	0.997	2.951	7.754	4.803	2.816	2.876
10	a-C_s	2.951	0.874	0.996	1.755	7.458	5.703	2.791	3.009
11	a-C_1	2.917	0.767	0.999	2.087	7.647	5.56	2.791	3.025
12	a-C_s	2.938	0.511	0.968	1.476	8.664	7.188	2.812	2.842

Cluster size (n)	symmetry	E_b(eV/atom)	ΔE (eV)	μ (μ_B)	VEA (eV)	VIP (eV)	η (eV)	$a_{Ge-Ge\ (Å)}$	$a_{Ga-Ge\ (Å)}$
13	a-C_s	2.988	0.611	0.999	2.457	7.424	4.967	2.776	2.861
14	a-C_1	2.997	0.666	0.999	2.259	7.569	5.31	2.804	3.039
15	a-C_s	3.027	0.653	0.990	2.240	8.132	5.892	2.796	2.992
16	a-C_s	3.037	0.900	0.999	1.829	7.109	5.28	2.809	3.071
17	a-C_1	2.992	0.497	0.935	1.884	7.765	5.881	2.740	3.019
18	a-C_1	2.997	0.553	0.997	2.658	7.159	4.501	2.784	3.112
19	a-C_1	2.996	0.709	0.974	2.607	6.916	4.309	2.761	2.621
20	a-C_1	3.022	0.367	0.971	2.304	7.217	4.913	2.691	2.928

All clusters with sizes n = 13, 14, 15, 16, and 17 provide prolate cages, where the Ga atom situated on the surface. The computed binding energies for the sizes of these clusters are much less than those for the corresponding pure germanium clusters.

As for larger clusters $GaGe_{18,\ 19,\ 20}$, the most appropriate geometry of each cluster is an irregular cage-like configuration. We can note that in the case of these clusters the values of binding energies are lower than those of the corresponding Ge_n clusters.

3.2. Electronic properties

3.2.1. Binding energy E_b

The relative stability of the studied clusters ($GaGe_n$) can be evaluated by discussing the binding energy (eV/atom), which is given by the following formula:

$$E_b(GaGe_n) = (n\,E(Ge) + E(Ga) - E(GaGe_n))/(n + 1) \quad (1)$$

where:

n: the size of the studied cluster.

E(Ge): the total energy of the free Ge atom.

E(Ga): the total energy of the free Ga doping atom.

$E(GaGe_n)$: the total energy of the studied cluster.

The calculation results for binding energy are given in Table 2. Fig. 2 shows a comparison of changes in the binding energy as a function of the size n for the most appropriate isomers of Ge_{n+1} and $GaGe_n$ clusters. Mostly, the binding energy increases constantly with increasing size n for both clusters, where the augmentation in the average number of neighbors per atom is can most probably be relating to that.

For $GaGe_n$, we note that the binding energy curve is lower than that for Ge_{n+1}, with the exception of the case $GaGe_5$ cluster. This means that the doping with the Ga atom generally has not reinforced the stability of germanium cages. So we can concluded that the $GaGe_5$ cluster very stable because it has a larger value of binding energy (3.148 eV/atom)

A rapid increase in binding energy was obtained from 1.219 eV/atom to 3.148 eV/atom for n = 1 and n = 5 respectively, while for the rest clusters sizes it has a slow and non-monotonous growth behavior.

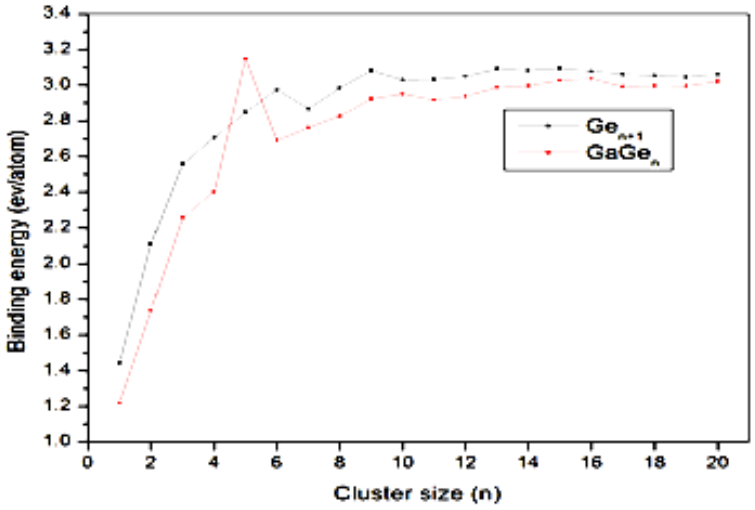

Fig. 2. Binding energy for the most appropriate structures of Ge_{n+1} and $GaGe_n$ (n = 1-20) clusters as a function of cluster size n (color online)

3.2.2. Fragmentation Energy E_f

In order to predict the relative stability of the clusters, we studied the fragmentation energy of the $GaGe_n$ clusters (n = 1–20). Its values are ordering in Table 2, which was calculated by using:

$$E_f(GaGe_n) = E(GaGe_{n-1}) + E(Ge) - E(GaGe_n) \quad (2)$$

In this equation $E(GaGe_{n-1})$ is the total energy of the $GaGe_{n-1}$ cluster.

Fig. 3 shows an oscillating behavior in the fragmentation energy evolution of each cluster size. The clusters Ge_5, Ge_8, Ge_{10}, Ge_{11}, Ge_{15}, $GaGe_3$, $GaGe_5$, $GaGe_9$, $GaGe_{13}$, and $GaGe_{20}$ have a higher thermodynamic stability pattern than their neighbors.

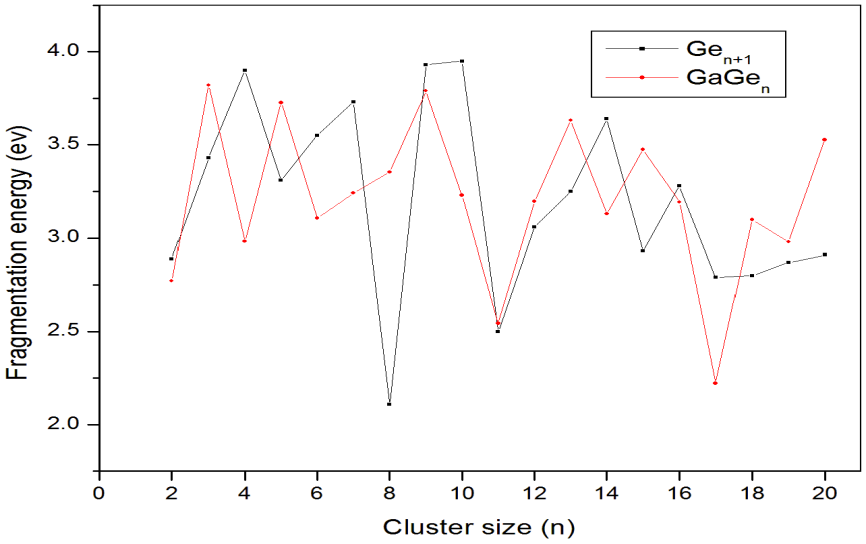

Fig. 3. Fragmentation energy for the most appropriate structures of Ge_{n+1} and $GaGe_n$ (n = 1–20) clusters as a function of cluster size n (color online)

3.2.3. Second-order difference Δ_2E

The second-order energy difference is a sensitive parameter in cluster physics that directly reflects the relative stability. It was can be obtained by relation:

$$\Delta_2E = E(GaGe_{n+1}) + E(GaGe_{n-1}) - 2\,E(GaGe_n) \quad (3)$$

where E is the total energy of the intended cluster. In Table 2 we displayed the results obtained for $GaGe_n$ (n = 1–20) clusters, and their variation in terms of the cluster size n was plotted in Fig. 4. We note from the curve, there are prominent positive peaks for the $GaGe_n$ structures at n = 2, 4, 6, 8, 11, 12, 14, 17, and 19 foretelling that these structures have higher stability property than their neighbors.

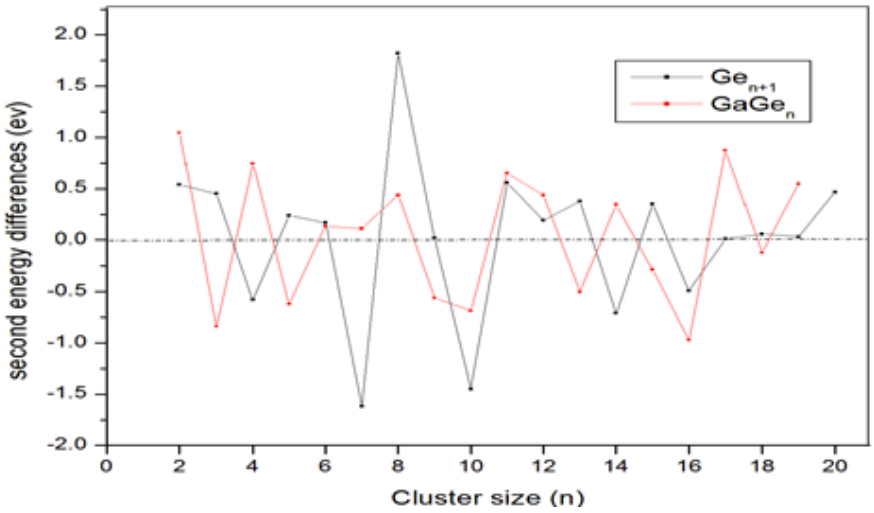

Fig. 4. Second-order difference for the most appropriate structures of Ge_{n+1} and $GaGe_n$ (n = 1–20) clusters as a function of cluster size n (color online)

3.2.4. HOMO–LUMO gap ΔE

We calculated the energy gap (ΔE) which is an important criterion in terms of the electronic stability of clusters and also represents the cluster's ability to participate in chemical reactions. The computed values of ΔE are listed in Table 2.

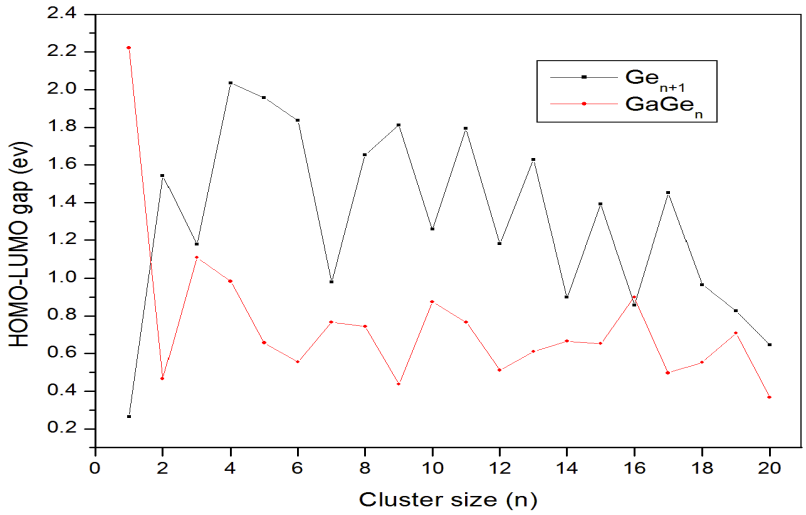

Fig. 5. HOMO-LUMO gap for the most appropriate structures of Ge_{n+1} and $GaGe_n$ (n = 1–20) clusters as a function of cluster size n (color online)

The results obtained for the most appropriate structures are plotted as a function of cluster size change as shown in Fig. 5, where from this figure, it can be remarked that the HOMO-LUMO gap values of $GaGe_n$ clusters are significantly lower than that of the pure Ge_{n+1} clusters, excluding for n = 1 and 16. It can be concluded that the replacement of one Ge by one atom of Ga increases the chemical activity of the host germanium

clusters. In addition, oscillations and non-monotonous behavior are observed of the HOMO-LUMO gaps that are tending in the decreasing direction for both $GaGe_n$ and Ge_{n+1} structures. It should also be noted that the $GaGe_1$ cluster has the eminent peak of HOMO-LUMO gap at a value 2.222 eV. This signifies that the $GaGe_1$ cluster has higher chemical stability and less active than its neighbors.

3.2.5. Vertical ionization potential (VIP) and vertical electronic affinity (VEA)

The vertical electron affinity and vertical ionization potential are substantial parameters for studying change in the electronic configuration of clusters and also for determining their stability.

The vertical electron affinity (VEA) and vertical ionization potential (VIP) are defined by the following equations:

$$VEA = E(GaGe_n) - E(GaGe_n^-) \quad (4)$$

$$VIP = E(GaGe_n^+) - E(GaGe_n) \quad (5)$$

where $E(GaGe_n^+)$ are the energy of the cationic clusters, and $E(GaGe_n^-)$ are the energy of the anionic clusters.

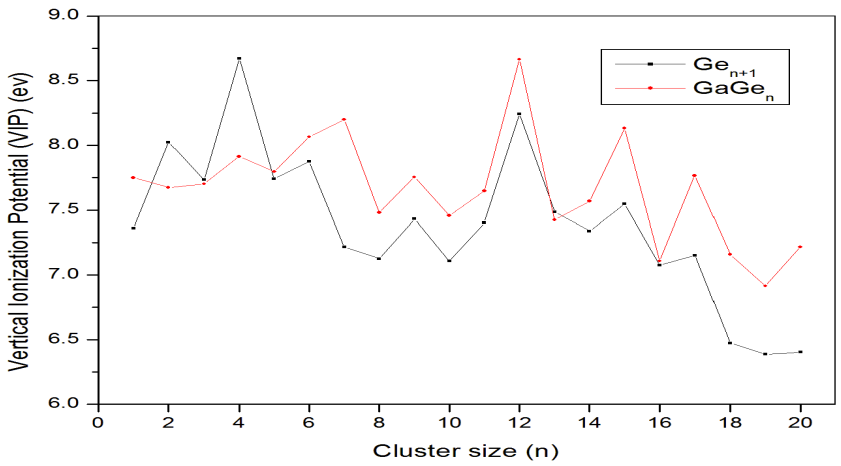

Fig. 6. Vertical ionization potential for the most appropriate structures of Ge_{n+1} and $GaGe_n$ (n = 1–20) clusters as a function of cluster size n (color online)

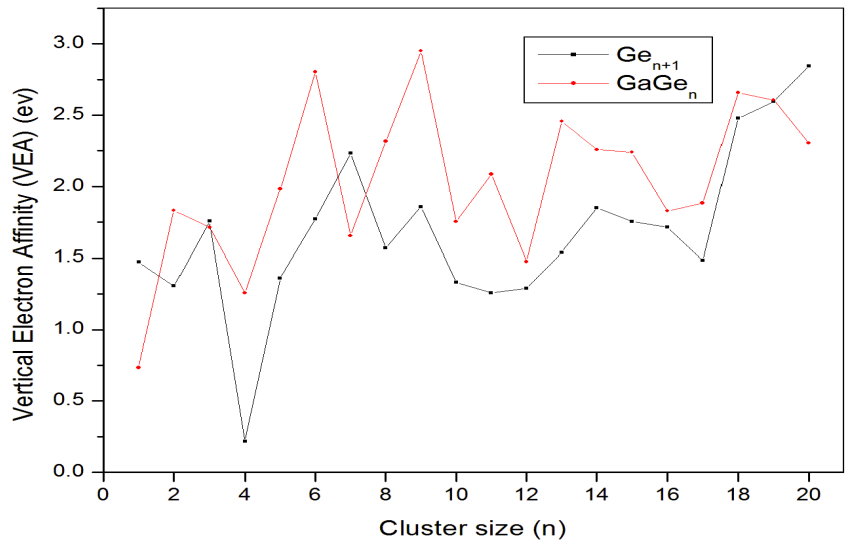

Fig. 7. Vertical electron affinity for the most appropriate structures of Ge_{n+1} and $GaGe_n$ (n = 1–20) clusters as a function of cluster size n (color online)

From the values of VIP and VEA which are in Table 2, we plotted the Figs.6 and 7, where we can see through those figures oscillating behavior in the evolution of VIP and VEA for both clusters of pure germanium and doped germanium by Ga atom.

We note that the VIP curve (Fig. 6) of $GaGe_n$ clusters is larger than that of Ge_{n+1}. This signifies that $GaGe_n$ clusters have a lower possibility for ionization and are therefore more steady, with the exception of small $GaGe_n$ clusters at n = 2–4 which are closer to the metallic character.

On the other hand, $GaGe_n$ clusters show a higher increasing evolution of VEA values compared to Ge_{n+1} clusters (Fig. 7), indicating that it will capture electrons more facilely, except the clusters at n = 1, 7, and 20.

3.2.6. Chemical hardness η

Based on the principle of maximum hardness (PMH) [34], the relative stability of small clusters can be distinguished by chemical hardness (η).

Chemical hardness is calculated by the following relation:

$$\eta = \text{VIP-VEA} \quad (6)$$

Fig. 8 shows a non-monotonic decreasing of the chemical hardness as a function of cluster size for both Ge_{n+1} and $GaGe_n$ (n = 1–20) structures.

It is important to mention that the clusters having high chemical hardness values are usually more stable and less reactive. Therefore, our calculation revealed that the cluster $GaGe_{12}$ is more stable ompared to neighboring clusters because it has the largest chemical hardness value of 7.188 eV (Table 2).

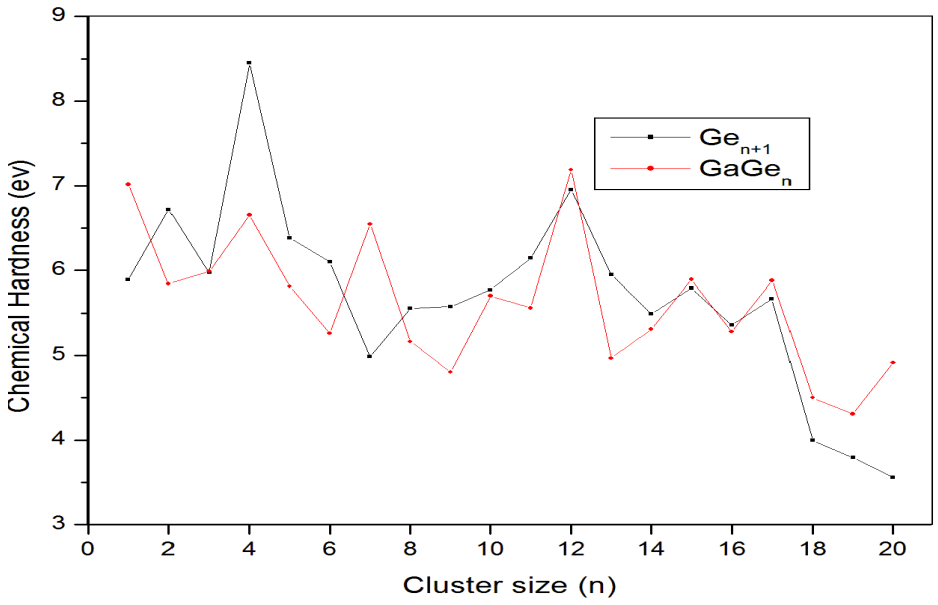

Fig. 8. Chemical hardness for the most appropriate structures of Ge_{n+1} and $GaGe_n$ (n = 1–20) clusters as a function of cluster size n (color online)

3.3. Magnetic properties

In order to discuss the magnetic properties, which are considered as a very important factor to study the behavior of the clusters especially those small sizes, we calculated the total spin magnetic moment (TSMM). Where the obtained values for this latter are tabulated in Table 1 for all $GaGe_n$ clusters. We can note that the TSMM values are in the range of $1\mu_B$ with the exception of the $GaGe_1$ small cluster which is estimated to be $3\mu_B$.

In Fig. 9, we plotted the total densities of states (DOS) and partial densities of states (PDOS) for the most suitable structure of $GaGe_1$ and $GaGe_2$ clusters (we take this cluster instead of the rest ones). From the PDOS in Fig. 9, the GaGe dimer gives the largest total spin

magnetic moment value of $3\mu_B$. This is due to the large contribution of 4p valence orbitals of both germanium and gallium atoms. This means that the $GaGe_1$ cluster can be used in many applications on the nanoscale.

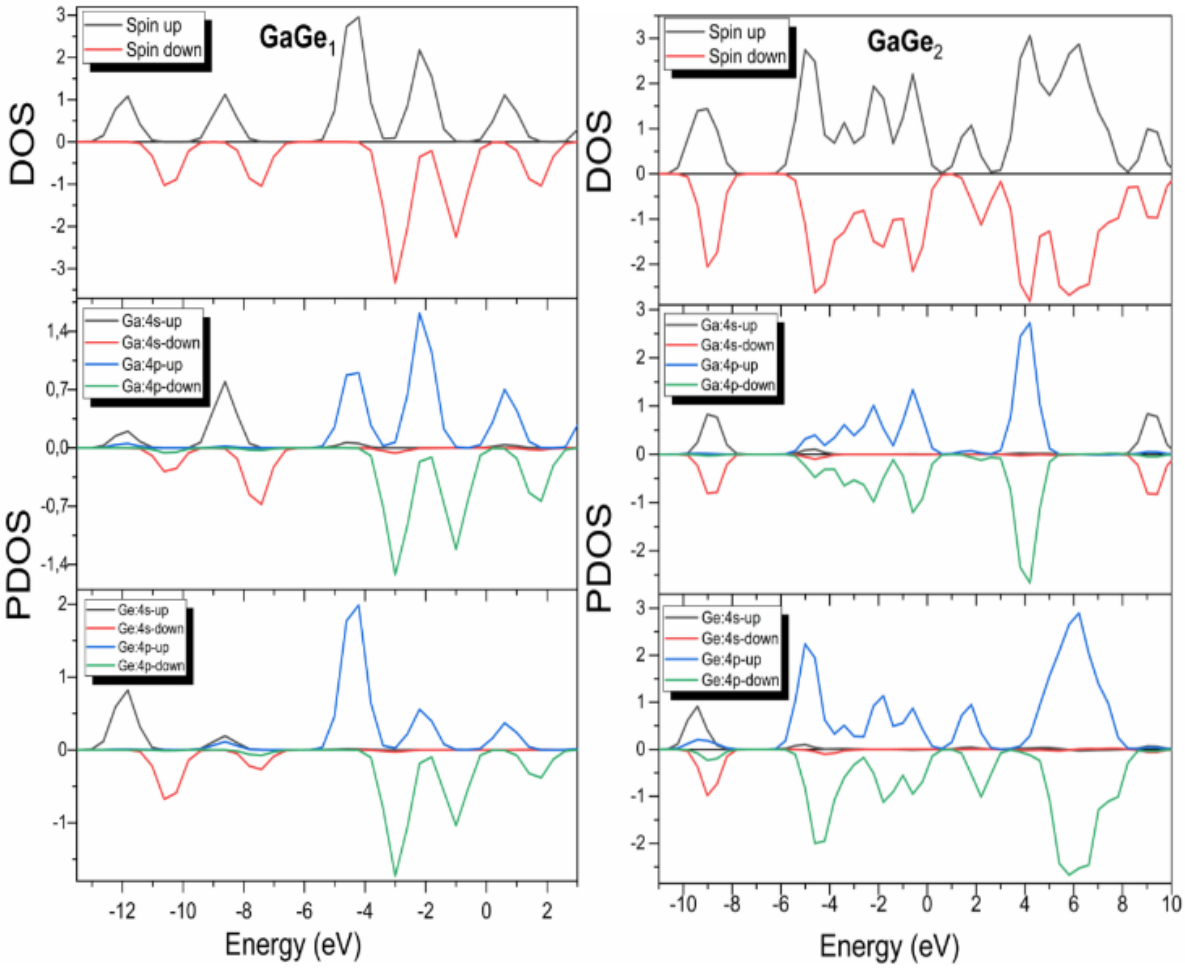

Fig. 9. The total and partial density of states for most appropriate structures of $GaGe_1$ and $GaGe_2$ clusters (color online)

4. Conclusion

Based on the DFT calculations, we proposed to study the doping of one gallium atom into the framework of pure germanium clusters to achieve the geometrical structures, electronic, and magnetic characteristics, and the results obtained (as E_b, E_f, Δ_2E, ΔE, VEA, VIP, η) are compared to that of the pure germanium clusters.

Our results indicate that the doping Ga atom favors stability on the germanium cage surface, for most stable clusters. The obtained second-order energy difference Δ_2E results show that the positive maximum peaks at n = 2, 4, 6, 8, 11, 12, 17, and 19 have private stability. Likewise, the fragmentation energy results reveal that the $Ge_{5,\ 8,\ 10,\ 11,\ 15}$ and $GaGe_{3,\ 5,\ 9,\ 13,\ 20}$ clusters have more thermodynamic stability than the others.

On the other hand, according to the HOMO-LUMO gaps analysis, we conclude that the GaGe clusters have lower HOMO-LUMO gap values than the corresponding pure germanium clusters, excluding for n = 1 and 16, suggesting that the substitution of one Ge atom by a Ga one enhances the chemical reactivity of the host germanium clusters, and thus increases the metallic character of relevant clusters.

Among the most appropriate clusters, the $GaGe_1$ cluster has the largest total spin magnetic moment value of $3\mu_B$.

The results of this work are very important in the field of stimulation and can give strong guidance for research on experimental level.

Acknowledgments

The authors would like to thank the members of LENREZA Laboratory, Department of Physics, Faculty of mathematics and material sciences, University Kasdi Merbah Ouargla, Algeria.

References

[1] G. Schmid, D. Fenske, Phil. Trans. R. Soc. A. **368**, 1207 (2010).
[2] K. D. Sattler, Handbook of nanophysics clusters and fullerenes, CRC, Boca Raton, 2017.
[3] N. Kapila, I. Garg, V. K. Jindal, H. Sharma, J. Magn. Magn. Mater. **324**(18), 2885 (2012).
[4] J. M. Hunter, J. L. Fye, M .F. Jarrold, J.E. Brower, Phys. Rev. Lett. **73**(2063), 15 (1994).
[5] S. Ogut, J. R. Chelikowsky, Phys. Rev. B. **55**(R4914), 8 (1997).
[6] X. J. Hou, G. Gopakumar, P. Lievens, M.T. Nguyen, J. Phys. Chem. A. **111**(51), 13544 (2007).
[7] I. Shim, M. S. Baba, K. A. Gingerich, Chem. Phys. **277**(1), 9 (2002).
[8] J. Wang, J. G. Han, Chem. Phys. **123**(24), 244303 (2005).
[9] W. J. Zhao, Y. X. Wang, Chem. Phys. **352**(1-3), 291 (2008).
[10] X. J. Deng, X. Y. Kong, X. L. Xu, H. G. Xu, W. J. Zheng, Chem. Phys. Chem. **15**(18), 3987 (2014).
[11] R. Trivedi, K. Dhaka, D. Bandyopadhyay, RSC. Adv. **4**(110), 64825 (2014).
[12] D. Jing, F. Tian, Y .Wang, J. Chem. Phys. **128**(12), 124319 (2008).
[13] A. D. Zdetsis, J. Phys. Chem. A, **113**(44), 12079 (2009).
[14] P. N. Samanta, K. K. Das, Comput. Theor. Chem. **980**, 123 (2012).
[15] X. Q. Liang, X. J. Deng, S. J. Lu, X. M. Huang, X. L. Xu, J. J. Zhao, W. J. Zheng, J. Phys. Chem. **121**(12), 7037 (2017).
[16] M. Benaida, K. E. Aiadi, S. Mahtout, S. Djaadi, W. Rammal, M. Harb, J. Semicond. **40**(3), 032101 (2019).
[17] S. Mahtout, Y. Tariket, Chem. Phys. **472**, 270(2016).
[18] S. Mahtout, C. Siouani, S. Safer, F. Rabilloud, J. Phys. Chem. A. **122**(2), 662 (2018).
[19] C. Siouani, S. Mahtout, S. Safer, F. Rabilloud, J. Phys. Chem. A. **121**(18), 3540 (2017).
[20] C. Siouani, S. Mahtout, S. Safer, J. Mol. Model. **25**(5), 113 (2019).
[21] L. Mustapha, S. Mahtout, F. Rabilloud, Comput. Theor. Chem. **1181**, 112830 (2020).
[22] J. M. Soler, E. Artacho, J. D. Gale, A. Garcia, J. Junquera, P. Ordejon, and D. Sanchez-Portal, J. Phys: Condens. Matt. 14(11), 2745 (2002).
[23] N. Troullier, J. L. Martins, Phys. Rev. B. **43**(3), 1993 (1991).
[24] P. Ordejón, E. Artacho, J. M. Soler, Phys. Rev. B **53**(16), R10441 (1996).
[25] J. P. Perdew, K. Burke, M. Ernzerhof, Phys. Rev. Lett. **77**(18), 3865 (1996).
[26] S. Nagendran, S. S. Sen, H. W. Roesky, D. Koley, H. Grubmüller, A. Pal, R. Herbst-Irmer, Organometallics **27**(21), 5459 (2008).
[27] J. Wang, G. Wang, J. Zhao, Phys. Rev. B. **64**(20), 205411 (2001).
[28] L. Lou, L. Wang, L. P. F. Chibante, R. T. Laaksonen, P. Nordlander, and R. E. Smalley, J. Chem. Phys. **94**(12), 8015 (1991).
[29] R. M. Graves, J. Chem. Phys. **95**(9), 6602 (1991).
[30] K. Balasubramanian, J. Phys. Chem. **90**(26), 6786 (1986).
[31] V. Sharma, A. Pahuja, S. Srivastava, Mol. Phys. **114**(9), 1472 (2016).
[32] N. Troullier, J. L. Martins, Phys. Rev. B **43**(3), 1993 (1991).
[33] J. Junquera, O. Paz, D. Sánchez-Portal, E. Artacho Phys. Rev. B **64**(23), 235111 (2001).
[34] R. G. Pearson, J. Chem. Sci. **117**(5), 369 (2005).

*Corresponding author: z.ikram30@gmail.com